Carbohydrate Polymers 104 (2014) 101–108

Contents lists available at ScienceDirect

Carbohydrate Polymers

journal homepage: www.elsevier.com/locate/carbpol

Water-induced shape-memory poly(D,L-lactide)/microcrystalline cellulose composites

Ye Liu, Ying Li, Hongmei Chen, Guang Yang, Xiaotong Zheng, Shaobing Zhou*

Key Laboratory of Advanced Technologies of Materials, Ministry of Education, School of Materials Science and Engineering, Southwest Jiaotong University, Chengdu, Sichuan 610031, PR China

ARTICLE INFO

Article history:
Received 30 November 2013
Received in revised form
24 December 2013
Accepted 10 January 2014
Available online 21 January 2014

Keywords:
Shape memory
Composites
Biodegradable
Microcrystalline cellulose

ABSTRACT

Thermo-induced shape-memory polymers (SMPs) have been widely investigated, but their biomedical applications are limited because their switching temperature does not fall completely within the range of room temperature to body temperature. In this study, we prepared water-induced shape-memory composites composed of microcrystalline cellulose (MCC) and poly(D,L-lactide) (PDLLA). We observed that the composite with an MCC content of 35% (PDLLA-MCC-35) exhibited a good shape-memory effect upon exposure to water at 37 °C. We also analyzed the mechanism of the water-triggered shape-memory effect by considering the microstructure, water contact angle, water uptake, thermal properties and static and dynamic mechanical properties of the composite. The results of in vitro degradation analysis demonstrate that the composites exhibited good biodegradation. In addition, Alamar blue assays based on osteoblasts indicate that the composites possess good cytocompatibility. Therefore, the water-induced shape-memory composite can potentially be developed into a new smart medical device.

1. Introduction

Shape-memory polymers (SMPs) are a class of stimuli-responsive materials (Lendlein & Kelch, 2002) that can be deformed and fixed into a temporary shape under specific stress conditions and subsequently recover their original shape upon exposure to an external stimulus, such as heat (Leng, Lan, Liu, & Du, 2011; Liu, Qin, & Mather, 2007; Lendlein & Langer, 2002; Ratna & Karger-Kocsis, 2008), light (Jiang, Kelch, & Lendlein, 2006; Lendlein, Jiang, Jünger, & Langer, 2005), electric field (Cho, Kim, Jung, & Goo, 2005; Luo & Mather, 2010; Liu, Lv, Lan, Leng, & Du, 2009; Xiao, Zhou, Wang, & Gong, 2010), magnetic field (Mohr et al., 2006; Schmidt, 2006; Yu et al., 2009; Zheng et al., 2009) or moisture (Chen, Hu, & Zhuo, 2011; Chen, Hu, Yuen, & Chan, 2009; Huang, Yang, An, Li, & Chan, 2005; Yang, Huang, Li, & Li, 2006; Yang, Huang, Li, Lee, & Li, 2004). SMPs are elastomers that consist of netpoints and suitable stimuli-sensitive switch units. The netpoints determine the permanent shape of an SMP, and the switch units are responsible for controlling shape fixity and recovery (Behl & Lendlein, 2007; Hu, Zhu, Huang, & Lu, 2012; Xie, 2011). Due to the various switch units that occur in SMPs, these polymers can be designed to respond to different external stimuli. Although various external stimuli can be used as a recovery trigger, the most widely studied SMPs are thermally induced SMPs. However, thermally induced SMPs are not always suitable for biomedical applications because their switching temperature does not fall completely within the range of room temperature to body temperature.

Water-induced SMPs may be used to resolve this issue due to the lower transition temperature exhibited by the polymers with water in the polymer matrix. Water-induced SMPs may be more suitable for biomedical application because shape recovery occurs upon exposure to body fluid; consequently, these polymers have received increasing attention in recent years. For example, Huang and co-workers were the first to report that moisture could trigger shape recovery in polyurethane shape-memory polymers (Huang et al., 2005; Yang et al., 2004). Leng and co-workers reported that styrene-based thermosetting SMPs could recover their original shape after being immersed in N,N-dimethylformamide (DMF) (Lv, Leng, Liu, & Du, 2008; Lv, Liu, Zhang, Leng, & Du, 2008). In 2010, a solvent-induced shape-memory effect based on a chemically cross-linked polyvinyl alcohol was reported (Du & Zhang, 2010). The shape-recovery mechanism of the SMPs mentioned above involves the diffusion of low-molecular-weight molecules into the polymer matrix, which act as plasticizers to reduce the transition temperature of the materials until shape recovery occurs (Behl & Lendlein, 2007; Leng, Lv, Liu, & Du, 2008).

Most recently, a new type of water-induced shape-memory polymer composite was produced by introducing rigid cotton cellulose nanowhiskers into a rubbery polyurethane matrix (Mendez

* Corresponding author. Tel.: +86 28 87634068; fax: +86 28 87634649.
E-mail addresses: shaobingzhou@swjtu.edu.cn, shaobingzhou@swjtu.cn, shaobingzhou@hotmail.com (S. Zhou).

0144-8617/$ – see front matter © 2014 Elsevier Ltd. All rights reserved.
http://dx.doi.org/10.1016/j.carbpol.2014.01.031

et al., 2011; Zhu et al., 2012). However, to the best of our knowledge, most water-induced SMPs are not biodegradable. In addition, the residual monomers in ester-based thermoplastic polyurethane water-induced SMPs may be harmful to body tissues.

The objective of the current study was to prepare biodegradable and biocompatible water-induced shape-memory composites by introducing microcrystalline cellulose (MCC) into a poly(D,L-lactide) (PDLLA) matrix. PDLLA is a thermoplastic aliphatic polyester that exhibits excellent biodegradation and biocompatibility. Furthermore, PDLLA is also a type of thermally induced SMP (Langer, Lendlein, Schmidt, & Grablowitz, 1999; Zheng, Zhou, Li, & Weng, 2006). However, PDLLA is not hydrophilic; thus, water cannot permeate the PDLLA matrix easily and quickly. To improve the wettability of PDLLA, we introduced MCC into the polymer matrix. Cellulose is the most abundant biopolymer found in nature and offers many advantages such as low cost, low density and biodegradability (de Souza Lima & Borsali, 2004; Klemm, Heublein, Fink, & Bohn, 2005). MCC is a novel form of commercial cellulose that exists as a fine, white, odorless, crystalline powder (Adel, El-Wahab, Ibrahim, & Al-Shemy, 2011; Das, Ray, Bandyopadhyay, & Sengupta, 2010). Furthermore, MCC exhibits great hygroscopicity (Ardizzone et al., 1999). Therefore, MCC has been widely used in different industrial fields, especially in the food, cosmetics and medical industries (El-Sakhawy & Hassan, 2007). To date, there is little work that has been published to describe the water-induced shape-memory properties of PDLLA/MCC composites.

2. Experimental

2.1. Materials

PDLLA (weight average molecular weight (Mw): 100 kDa, number average molecular weight (Mn): 72.8 kDa) was synthesized by the ring-opening polymerization of D,L-lactide monomer as described previously (Deng, Zhou, Li, Zhao, & Yuan, 2001). The molecular weight was measured using a Waters 2695/2414 Gel Permeation Chromatograph (GPC, Waters, America) and a Styragel HT4DMF column calibrated with polystyrene standards operated at 40 °C and series 2414 refractive index detector. MCC was purchased from Chengdu Reagent Factory. The average size of MCC determined using a laser scattering particle size diffraction analyser (Horiba, LA-920, Japan) was 25 μm. All other chemicals and solvents were of reagent grade or better.

2.2. Preparation of PDLLA/MCC composites

PDLLA/MCC composites were prepared by a solution casting method as follows. First, the MCC was dispersed in chloroform at a concentration of 0.5 mg/mL and mixed vigorously in an ultrasonic bath. Subsequently, the solution containing the MCC was slowly dropped into the previously prepared PDLLA solution under stirring. The mixed solutions were stirred vigorously to obtain a homogeneous suspension. Subsequently, the PDLLA/MCC suspensions were transferred to Teflon molds and dried under vacuum. Finally, the completely dried composites were press-molded at 100 °C for 5 min in a mold. Three different compositions of the PDLLA/MCC composites were prepared and coded as PDLLA-MCC-25, PDLLA-MCC-30 and PDLLA-MCC-35; the numerical values indicate the contents of MCC in the composites were 25, 30 and 35 wt.%, respectively.

2.3. Characterization

The microstructures of specimens were investigated using a Quanta200 Scanning Electron Microscope (SEM, FEI, USA). Specimens were mounted and then coated with gold. The accelerating voltage and magnification level were 20.0 kV and 1000× respectively.

The water contact angle was measured with contact angle equipment (DSA 100, KRUSS, Germany) using the sessile drop method at room temperature. All contact angle data represent the averages of five measurements obtained at different locations of the sample surfaces.

The water uptake of the samples was calculated by measuring the samples' weight before and after immersion in deionised water at 37 °C. The weight ratio of absorbed water was calculated according to the following formula: $m_1 - m_0/m_0$, where m_1 is the weight of the sample after being immersed in water at 37 °C and m_0 is the weight of the sample before immersion in water.

Differential scanning calorimetry (DSC) measurements were performed on a TA DSC-Q100 under a nitrogen atmosphere. Samples immersed in water at 37 °C for 3 min were dried gently using tissue paper. Measurements were carried out from 0 to 80 °C at a heating rate of 10 °C min^{-1}.

The tensile properties of the samples at room temperature were measured using an Instron 5567 (Instron Co., MA) instrument. The extension rate was 1 mm min^{-1}, and the initial gauge length was 32 mm.

The dynamic mechanical properties of the pure PDLLA and composites were determined on a TA DMA-Q 800 Instrument using the tensile resonant mode from 0 to 80 °C at a heating rate of 3 °C min^{-1}. The measurements were performed at a constant frequency of 1 Hz. Samples immersed in water at 37 °C for 3 min were dried gently using tissue paper. The test specimen dimensions were 30 mm × 4 mm × 0.15 mm (length × width × thickness).

The water-induced shape-memory effect was measured as follows. First, the rectangular strip samples were folded by deforming at 68 °C and fixed by cooling to room temperature. Second, the fixed samples were immersed in water and in air at 37 °C, respectively. Then, images of the shape recovery were recorded using a video camera. In the present work, the recovery ratio was defined as $[(\theta - \theta_0)/(180 - \theta_0)] \times 100$, where θ refers to the angle of the folded specimen at a given time at 37 °C and θ_0 indicates the angle at 0 min. The results represent the averages of at least three specimens. The samples were rectangular strip films with dimensions of 30 mm × 4 mm × 0.15 mm (length × width × thickness).

2.4. In vitro biodegradation

An in vitro biodegradation test was carried out in phosphate buffered saline (PBS) solution at pH = 7.4 at 37 °C. Briefly, all of the samples were cut into small round flakes with a diameter of nearly 20 mm and a thickness of 0.2 mm. Each specimen was accurately weighed and immersed in 15 mL PBS solution in a test tube. The tubes were kept in a thermo-stated shaking air bath that was maintained at 37 °C and operated at 100 cycles/min. After a certain period, the samples were taken out, rinsed several times with distilled water to remove residual buffer salts and dried to a constant weight in a vacuum desiccator. The degree of degradation was calculated according to the following formula: Weight loss (%) = $W_0 - W_t/W0 \times 100$, where W_0 is the dry weight before degradation and W_t is the dry weight at time t. The pH of the PBS solution was also measured. The results regarding the weight loss and the pH value are the averages of at least three specimens. Furthermore, the molecular weight was measured using a Waters 2695/2414 Gel Permeation Chromatograph (GPC, Waters, America).

2.5. Cytotoxicity analysis

Cytotoxicity was evaluated by Alamar blue assay as in our previous report (Shao et al., 2011). Briefly, all of the samples were

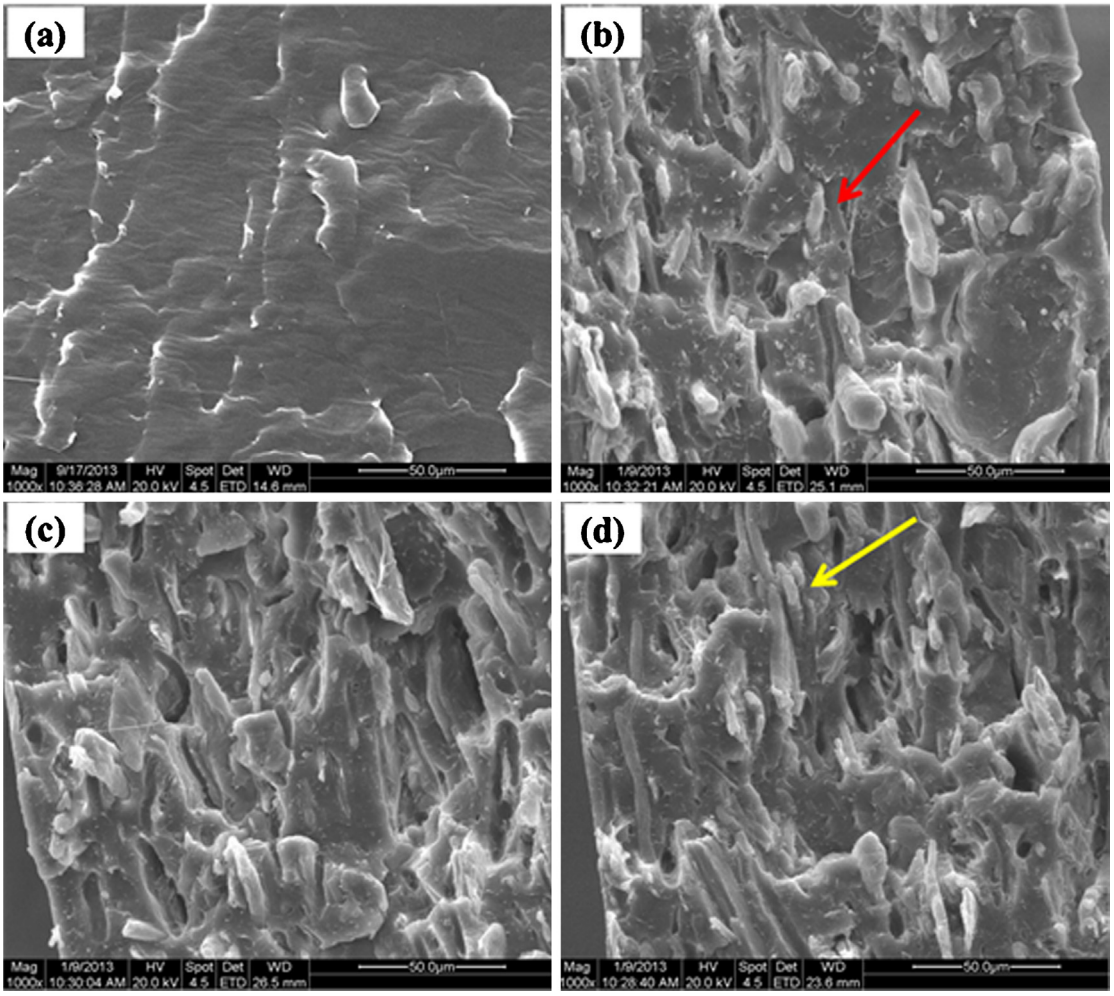

Fig. 1. A cross-sectional SEM image showing microstructure of pure PDLLA and PDLLA/MCC composites: (a) pure PDLLA; (b) PDLLA-MCC-25; (c) PDLLA-MCC-30; (d) PALLA-MCC-35.

cut into small round flakes with an average diameter of approximately 12 mm and sterilized by immersing in ethanol (75%) for 2 h. Then, the samples were used for osteoblasts culturing in vitro after remaining in sterilized PBS overnight. The cells were maintained in α-modified essential medium (α-MEM) (HyClone, USA) with 10% fetal bovine serum (FBS). The cells were inoculated on the samples and a tissue culture plate (control) with a density of 1×10^4 cells/well in 24-well tissue culture plates (Sigma–Aldrich) and grown at 37 °C in a 5% CO_2 humidified environment for 1, 3 and 5 days. After the incubation, the culture medium in each well was removed, and 300 μL Alamar blue solution (10% Alamar blue, 80% media 199 (Gibcos) and 10% FBS; v/v) was added into each well; the samples were then incubated for another 3 h. Wells without cells were used as blank controls. Samples of 200 μL of reduced Alamar blue solution were then removed for spectrophotometric absorbance measurements read at 570 (excitation)/600 (emission) using an ELISA microplate reader (Molecular Devices, Sunnyvale, CA). The cell viability ratio (R) for every sample was calculated using the equation R = (cell viability in experiment)/(cell viability in negative control). Cell morphology was evaluated by fluorescence microscopy (DMIL, Leica, Germany). The live osteoblast cells grown on samples for 1 and 5 days were stained by a 5% (v/v) calcein solution (diluted by PBS) for approximately 5 min and observed by fluorescence microscopy immediately.

3. Results and discussion

3.1. Morphology of the pure PDLLA and PDLLA/MCC composites

Cross-sections of the fractured samples, including the pure PDLLA and composites, were studied by scanning electron microscopy (SEM). Fig. 1a shows that the fractured surface of the pure PDLLA was smooth. Fig. 1b demonstrates that MCC (as indicated by the red arrow) was dispersed well and uniformly in the PDLLA matrix. However, with increasing MCC content, a few small aggregations (as indicated by the yellow arrow) were observed, as shown in Fig. 1d; MCC also showed good dispersion in the PDLLA matrix. The results indicate that we successfully prepared PDLLA/MCC composites with MCC dispersing well and uniformly.

3.2. Contact angle and water absorption analysis

To verify the change in the hydrophilicity of the composites after adding MCC, the water contact angle of the pure PDLLA and PDLLA/MCC composites was measured, as shown in Fig. 2a. The results indicate that the composites exhibited a lower contact angle than that of pure PDLLA. Pure PDLLA showed a contact angle of 83.5° in water, whereas the water contact angle of the PDLLA-MCC-35 composite decreased to 65.4°. This result indicates that the wettability of the PDLLA matrix was improved and also suggests that MCC

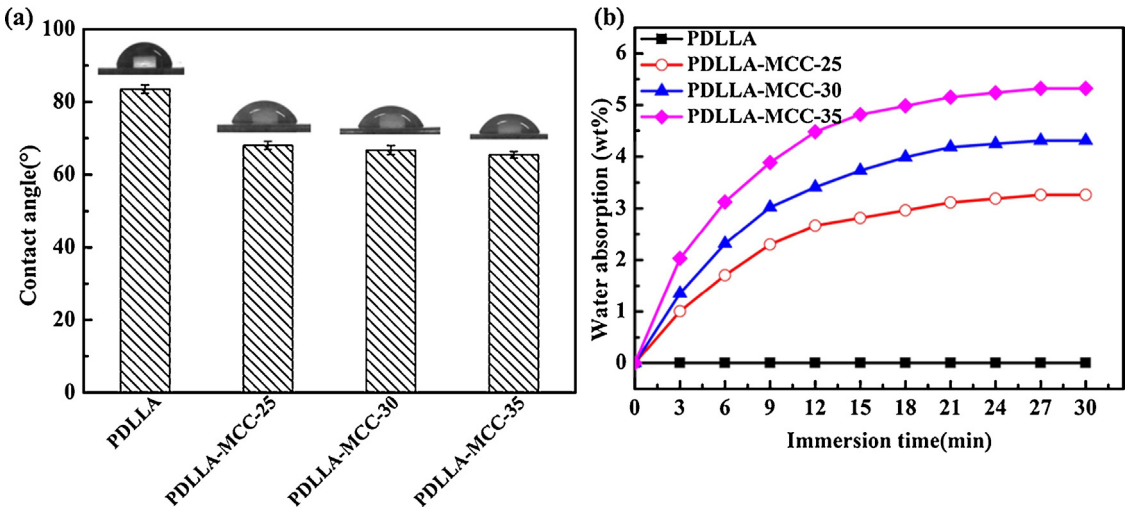

Fig. 2. (a) Water contact angle of the pure PDLLA and PDLLA/MCC composites. (b) Ratio of absorbed water to sample weight vs. immersion time.

was successfully incorporated into the PDLLA matrix. These results may have been due to the great hygroscopicity of MCC, which features an abundance of surface hydroxyl groups (Ardizzone et al., 1999).

Fig. 2b displays the water fraction in weight % in the PDLLA matrix vs. immersion time at 37 °C. It can be observed that the pure PDLLA exhibited no water absorption due to its high hydrophobicity, whereas the composites absorbed more and more water with increasing MCC content. In addition, the maximum absorbed water content of 5.32% was obtained for the PDLLA-MCC-35 composite. Finally, all of the composites tended to reach their saturated state after 30 min of immersion in water. This result suggests that the water absorption is dependent on the MCC content, where a higher MCC content results in a higher extent of water absorption. This effect may contribute to the increased wettability of the PDLLA matrix by the introduction of MCC.

3.3. Effect of water on glass transition temperature of PDLLA

The effect of water absorption on the T_g of PDLLA was also investigated using DSC analysis. Fig. 3 shows the DSC results of the pure PDLLA and PDLLA/MCC composites before and after immersion in water at 37 °C for 3 min. As shown, the T_g of pure PDLLA was approximately 55 °C, and the introduction of MCC into PDLLA had little effect on the T_g of pure PDLLA in the dry state. However, the T_g of all of the PDLLA/MCC composites dropped to below 37 °C after absorbing a certain amount of water. Additionally, with more water absorbed into the composites, the decrease in T_g became more significant, which is mainly ascribed to the fact that a certain amount of water that diffused into the PDLLA matrix acted as a plasticizer and reduced the T_g of the polymer, which is consistent with previous reports (Blasi, D'Souza, Selmin, & DeLuca, 2005; Paakinaho et al., 2012; Passerini & Craig, 2001).

3.4. Mechanical properties of the pure PDLLA and PDLLA/MCC composites

Fig. 4 shows typical stress–strain curves for the pure PDLLA and PDLLA/MCC composites. The tensile properties demonstrate that both the tensile stress and elongation to break clearly decreased as the MCC content increased. The decrease in tensile stress and elongation to break may be attributed to the low aspect ratio of MCC (Eichhorn & Young, 2001). However, with the increase in MCC content, the composites exhibited greater stiffness than the pure PDLLA, which may have been caused by the lower deformation capacity of the PDLLA/MCC composites.

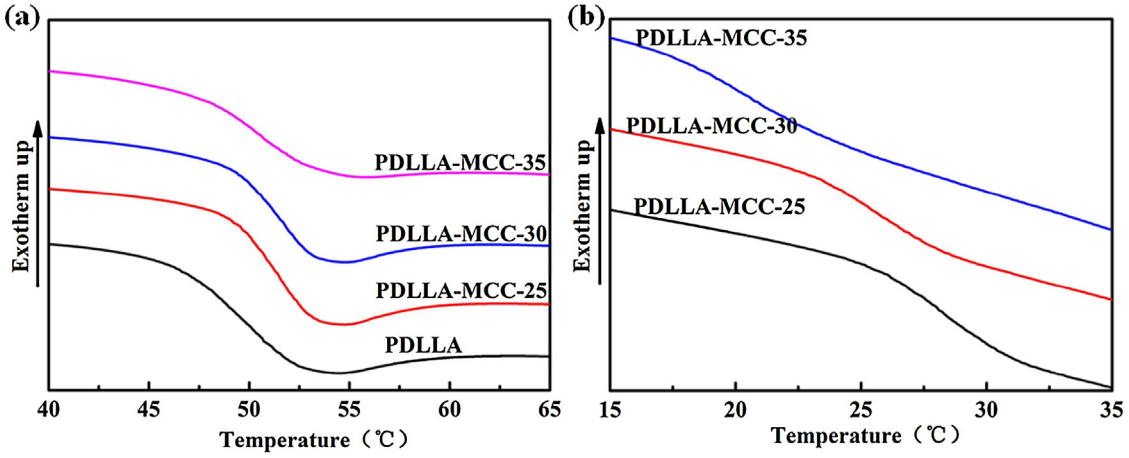

Fig. 3. DSC results of the pure PDLLA and PDLLA/MCC composites (a) before being immersed in water (b) after being immersed in water at 37 °C for 3 min.

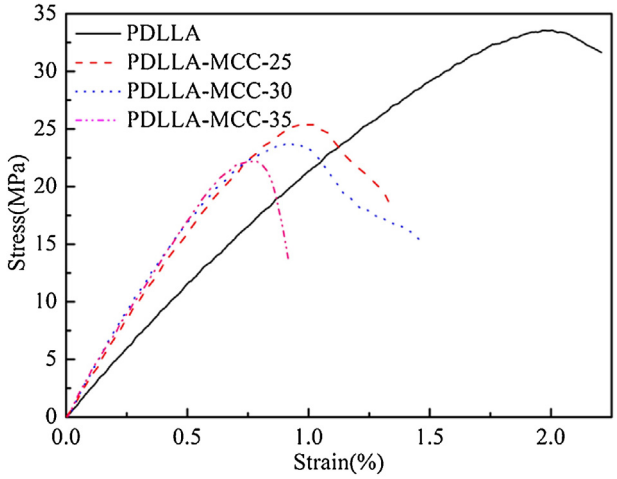

Fig. 4. Typical stress–strain curves of the pure PDLLA and PDLLA/MCC composites.

3.5. Dynamic mechanical properties of the pure PDLLA and PDLLA/MCC composites

Fig. 5 shows the storage modulus and tan delta curves of the pure PDLLA and PDLLA/MCC composites as a function of temperature. Fig. 5a shows that with the increase in MCC content, the storage modulus of the composites clearly increased both in the glassy state and in the rubbery state. For example, the storage modulus of the pure PDLLA was 2711 MPa at 30 °C, whereas the storage modulus of PDLLA-MCC-35 composite increased to 5275 MPa at 30 °C, an enhancement of 95%. Moreover, the storage modulus of the PDLLA-MCC-35 composite at 60 °C was 124 MPa, which represents a 1450% enhancement relative to the storage modulus of pure PDLLA. A high glassy-state modulus would provide the material with a high shape fixity upon cooling, whereas a high rubbery modulus would lead to a large elastic recovery at high temperature (Ratna & Karger-Kocsis, 2008). Shape-memory materials have to be designed to meet the abovementioned properties (Kim, Lee, & Xu, 1996; Liu, Gall, Dunn, & McCluskey, 2004). Based on these guidelines, it can be concluded that the PDLLA-MCC-35 composite exhibits the best shape-memory effect among all of the composites in the dry state.

With increasing MCC content, a significant decrease in the intensity of the tan delta peak can be observed in Fig. 5b. This decrease indicates that a specific interaction between the PDLLA matrix and MCC restricts the segmental mobility of the polymer chains in the composites (Jonoobi, Harun, Mathew, & Oksman, 2010; Wu, Henriksson, Liu, & Berglund, 2007). The specific interaction and the entangled MCC content may act as a physical cross-link and enhance the shape-memory property of the PDLLA matrix.

Fig. 5c shows the storage modulus of the PDLLA-MCC-35 composite after being immersed in water at 37 °C for 3 min. As shown, the T_g of the PDLLA-MCC-35 composite dropped to below 37 °C after absorbing some water, which is consistent with the results of DSC analysis. In addition, the composite retained a high storage modulus in the rubbery state after absorbing some water. The results indicate that the PDLLA-MCC-35 composite exhibits large elastic recovery at 37 °C in the wet state (Ratna & Karger-Kocsis, 2008).

3.6. Water-induced shape-memory effect of the pure PDLLA and PDLLA/MCC composites

Fig. 6a and b shows the shape-recovery behavior of the pure PDLLA and PDLLA/MCC composites in the dry state and in the wet

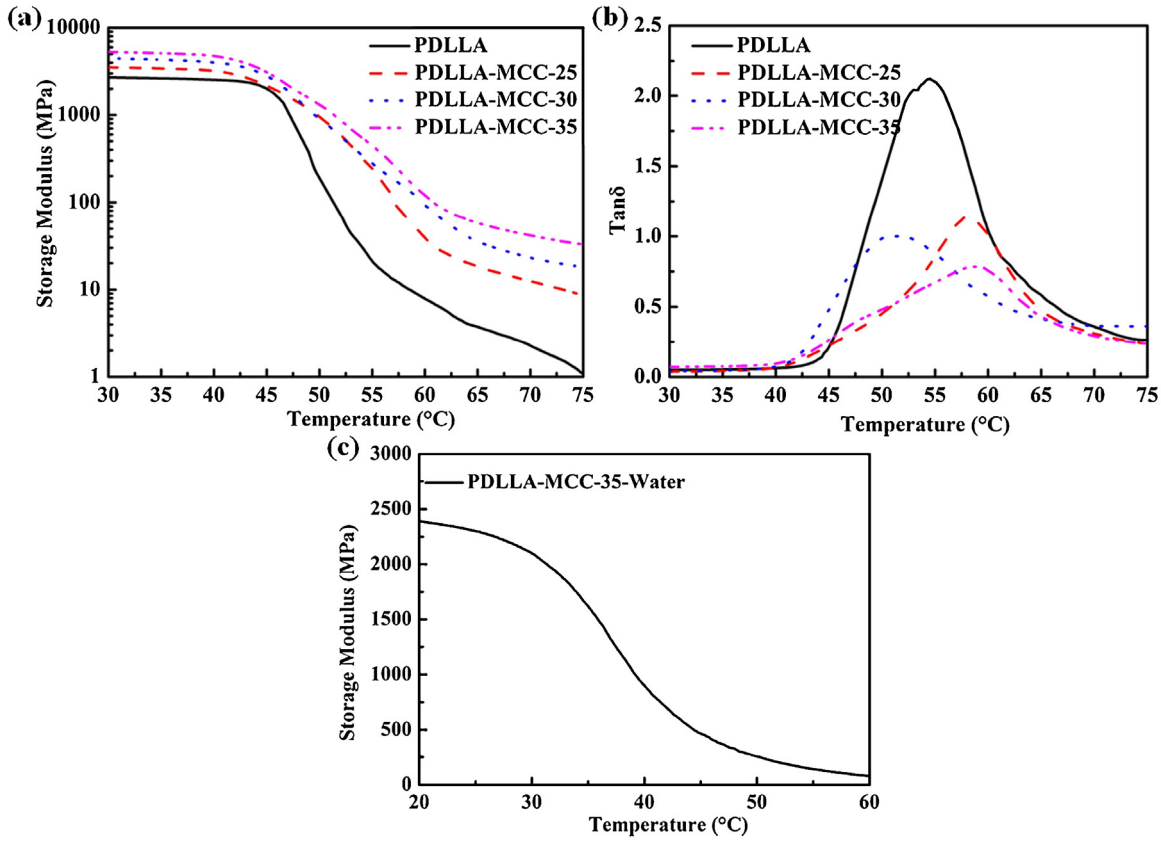

Fig. 5. DMA analysis of the pure PDLLA and PDLLA/MCC composites: (a) storage modulus; (b) tan δ curves; and (c) storage modulus of PDLLA-MCC-35 composite after being immersed in water at 37 °C for 3 min.

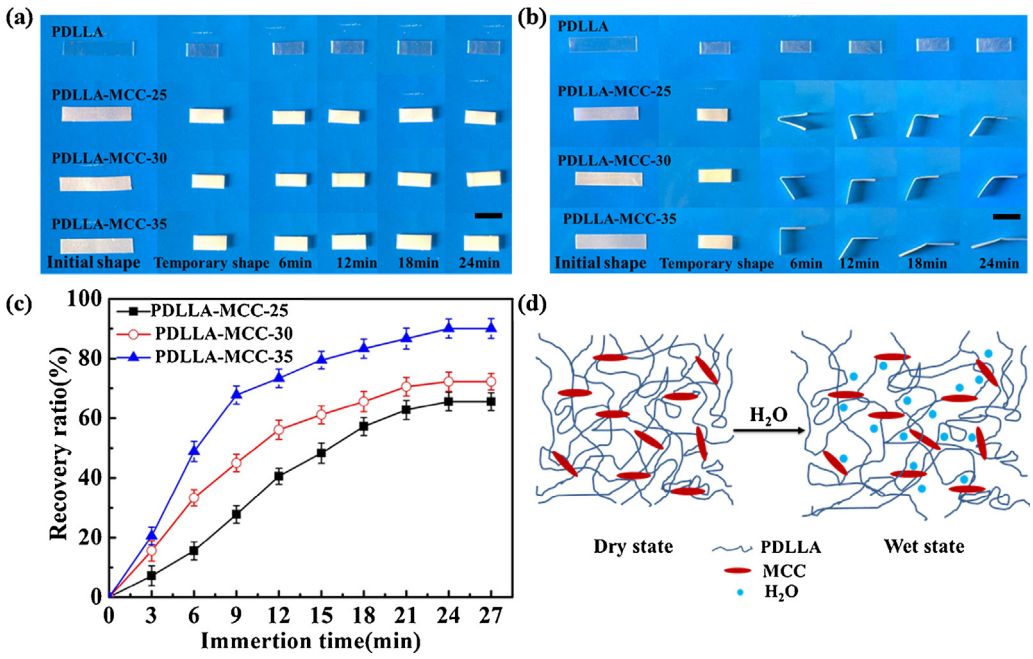

Fig. 6. (a) The shape-memory effect of the pure PDLLA and PDLLA/MCC composites in the dry state at 37 °C. (b) The shape-memory effect of the pure PDLLA and PDLLA/MCC composites in the wet state at 37 °C. (c) Shape-recovery ratio as a function of time for the PDLLA/MCC composites in the wet state at 37 °C. (d) Water-induced shape-memory mechanism of the PDLLA/MCC composites. All of the scale bars represent 10 mm.

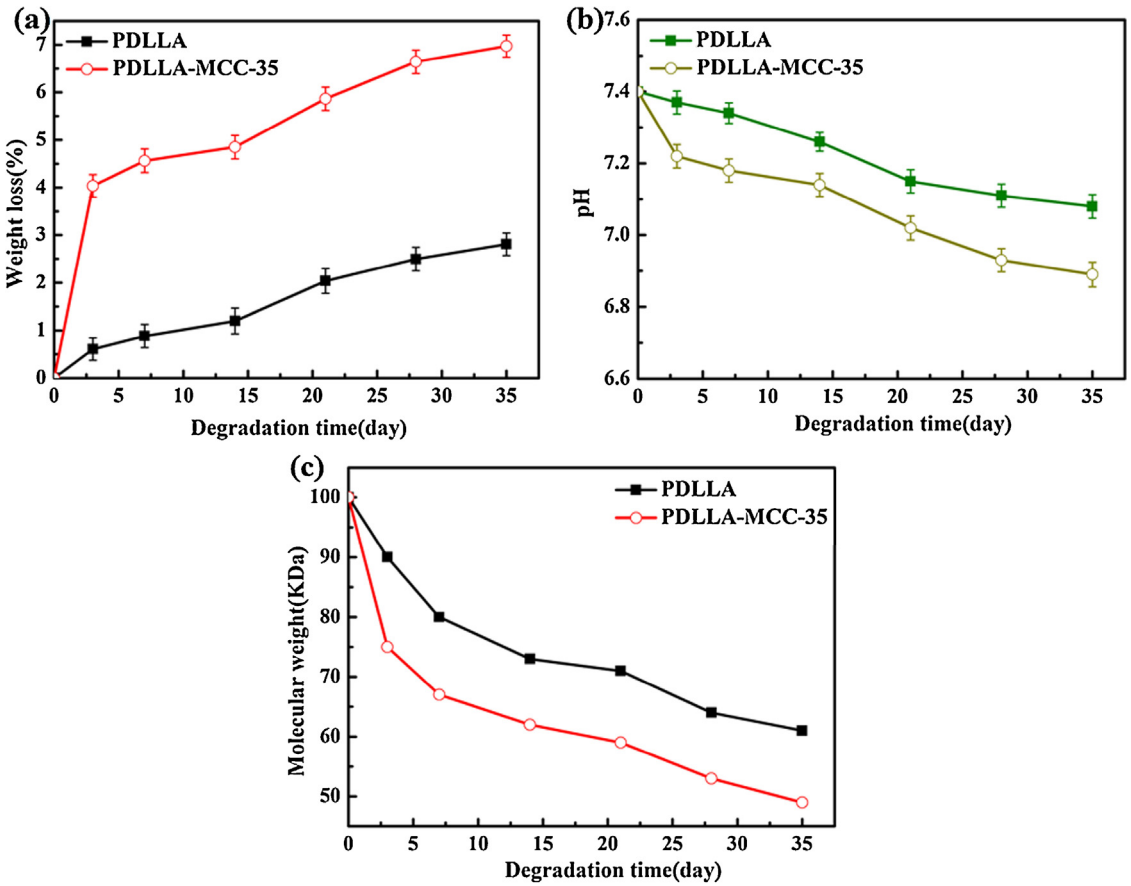

Fig. 7. (a) Weight loss percentages of pure PDLLA and the PDLLA-MCC-35 composite; (b) pH change in pure PDLLA and the PDLLA-MCC-35 composite; (c) molecular weight change in pure PDLLA and the PDLLA-MCC-35 composite.

state at 37 °C, respectively. It can be observed that all of the samples retained their temporary shape and showed no shape recovery in the dry state at 37 °C; however, when immersed in water at 37 °C, the composites demonstrated different degrees of recovery, and the pure PDLLA still retained its temporary shape. These results indicate that the samples could not recover their initial shape at 37 °C without the stimulus of water, which is attributed to the fact that in the wet state some absorbed water in the composites acts as a plasticizer and reduces the T_g of the composites until shape recovery occurs (Behl & Lendlein, 2007; Leng et al., 2008). Consequently, the shape recovery of the composites occurs under the stimulus of water at 37 °C. These composites can be used in vivo as smart biomedical devices with a capacity for shape recovery induced by body fluid.

The shape-recovery ratio as a function of time for the PDLLA/MCC composites is shown in Fig. 6c. It can be observed that the PDLLA-MCC-35 composite exhibited the highest shape-recovery speed and the best shape-recovery ratio. The results can be ascribed to the fact that in the wet state the PDLLA-MCC-35 composite exhibited a lower T_g, as shown in Fig. 3b, and a higher rubbery modulus, as shown in Fig. 5c. Consequently, the PDLLA-MCC-35 composite exhibited good shape-memory effects under the stimulus of water at 37 °C.

The proposed water-induced shape-memory mechanism for the PDLLA/MCC composites is shown in Fig. 6d. In the wet state, some water diffuses into the PDLLA/MCC composites matrix and act as a plasticizers, which leads to the slight swelling of the composites. The swelling effect induced in the polymer chains by the water molecules causes an increase in the flexibility of the macromolecular chains and a decrease in the T_g of the composites until shape recovery occurs. These phenomena obey the continuum theories of rubber elasticity, the Mooney-Rivlin equation and volume change refinement theory (Lu, Liu, Leng, & Du, 2010; Leng et al., 2011).

3.7. In vitro degradation analysis

The in vitro degradation behaviors of pure PDLLA and the PDLLA-MCC-35 composite are shown in Fig. 7. It can be observed that the weight loss increased and the pH of the PBS solution decreased with increasing degradation time for all samples. In addition, the molecular weight of both pure PDLLA and the PDLLA-MCC-35 composite decreased with increasing degradation time. This result is observed because the ester bonds in the PDLLA backbone were hydrolysed. It can also be observed that the degradation rate of the PDLLA-MCC-35 composite was significantly higher than that of pure PDLLA, which indicates that the biodegradation of the PDLLA matrix was enhanced by MCC due to an increase in the hydrophilicity of the polymer matrix.

3.8. Cytotoxicity analysis

The in vitro cytotoxicity of pure PDLLA and the PDLLA-MCC-35 composite assessed by measuring the viability of osteoblast cells is shown in Fig. 8a. It can be observed that for all groups the cell viability remained greater than 85%. Furthermore, the viability of osteoblast cells cultured on the PDLLA-MCC-35 composite was not significantly different from that of the cells cultured on pure PDLLA. This result indicates that introducing MCC into the PDLLA matrix has no cytotoxic effect on PDLLA, demonstrating the good biocompatibility of the PDLLA-MCC-35 composite in vitro. In addition, the morphology of the osteoblast cells cultured on pure PDLLA and the PDLLA-MCC-35 composite were observed by fluorescence microscopy after being stained by calcein. As shown in Fig. 8b, the osteoblast cells were able to establish a normal and healthy cell morphology on all samples. These results suggest that pure PDLLA and the PDLLA-MCC-35 composite presented good cytocompatibility.

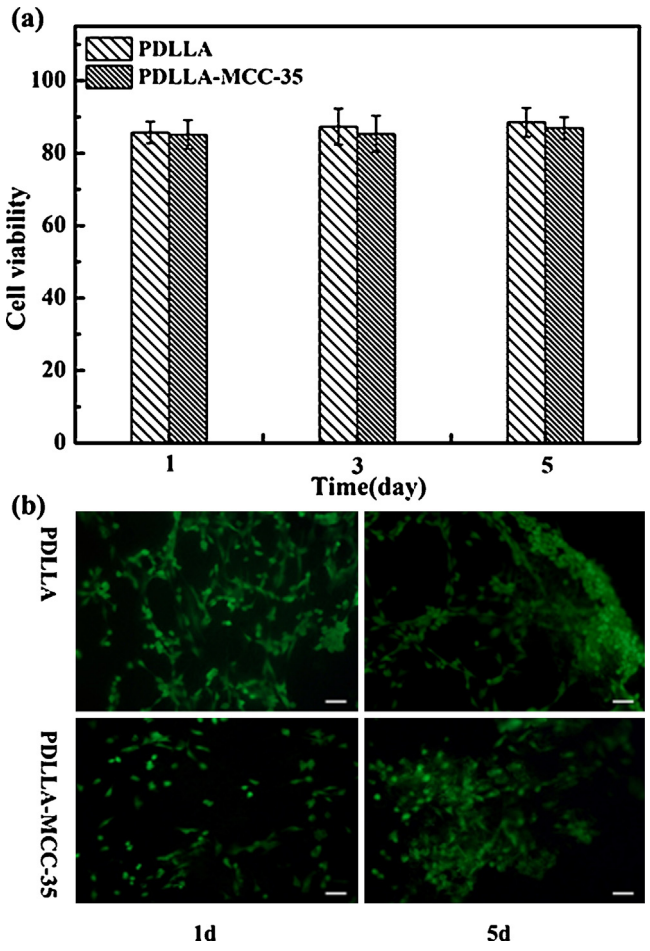

Fig. 8. (a) Cytotoxicity of osteoblasts cells cultured on pure PDLLA and the PDLLA-MCC-35 composite. (b) Fluorescence microscope images of osteoblasts cells cultured on pure PDLLA and the PDLLA-MCC-35 composite for 1 and 5 days, respectively. All of the scale bars represent 100 μm.

4. Conclusions

In this study, we successfully prepared water-induced shape-memory composites by introducing MCC into a PDLLA matrix. Unlike a thermo-induced shape-memory material, the composite containing 35% MCC exhibited a good shape-memory effect under the stimulus of water at 37 °C. The mechanism of this phenomenon is such that with the addition of MCC to the hydrophobic PDLLA matrix, a certain amount of water diffuses into the PDLLA/MCC composites in the wet state and acts as a plasticizer, which increases the flexibility of the macromolecular chains and reduces the T_g of the composite until shape recovery occurs. Moreover, in vitro biodegradation tests and cytotoxicity analysis demonstrated that the composite exhibits good biodegradation and biocompatibility. Therefore, the water-induced shape-memory composites developed in this study are especially attractive for potentially biomedical applications, such as self-tightening sutures and self-retractable and removable stents.

Acknowledgments

This work was partially supported by National Basic Research Program of China (973 Program, 2012CB933600), National Natural Science Foundation of China (51173150, 51203130, 51373138),

National Key Project of Scientific and Technical Supporting Programs Funded by MSTC (2012BAI17B06), Research Fund for the Doctoral Program of Higher Education of China (20120184110029) and Fundamental Research Funds for The Central Universities (SWJTU11ZT10, 2682013CX001).

References

Adel, A. M., El-Wahab, Z. H. A., Ibrahim, A. A., & Al-Shemy, M. T. (2011). Characterization of microcrystalline cellulose prepared from lignocellulosic materials. Part II: Physicochemical properties. *Carbohydrate Polymers*, *83*, 676–687.

Ardizzone, S., Dioguardi, F., Mussini, T., Mussini, P., Rondinini, S., Vercelli, B., et al. (1999). Microcrystalline cellulose powders: Structure, surface features and water sorption capability. *Cellulose*, *6*, 57–69.

Behl, M., & Lendlein, A. (2007). Shape-memory polymers. *Materials Today*, *10*, 20–28.

Blasi, P., D'Souza, S. S., Selmin, F., & DeLuca, P. P. (2005). Plasticizing effect of water on poly (lactide-co-glycolide). *Journal of Controlled Release*, *108*, 1–9.

Chen, S. J., Hu, J. L., Yuen, C.-w., & Chan, L. (2009). Novel moisture-sensitive shape memory polyurethanes containing pyridine moieties. *Polymer*, *50*, 4424–4428.

Chen, S. J., Hu, J. L., & Zhuo, H. T. (2011). Study on the moisture absorption of pyridine containing polyurethane for moisture-responsive shape memory effects. *Journal of Materials Science*, *46*, 6581–6588.

Cho, J. W., Kim, J. W., Jung, Y. C., & Goo, N. S. (2005). Electroactive shape-memory polyurethane composites incorporating carbon nanotubes. *Macromolecular Rapid Communications*, *26*, 412–416.

Das, K., Ray, D., Bandyopadhyay, N., & Sengupta, S. (2010). Study of the properties of microcrystalline cellulose particles from different renewable resources by XRD, FTIR, nanoindentation, TGA and SEM. *Journal of Polymers and the Environment*, *18*, 355–363.

de Souza Lima, M. M., & Borsali, R. (2004). Rodlike cellulose microcrystals: Structure, properties, and applications. *Macromolecular Rapid Communications*, *25*, 771–787.

Deng, X. M., Zhou, S. B., Li, X. H., Zhao, J., & Yuan, M. L. (2001). In vitro degradation and release profiles for poly-DL-lactide-poly(ethylene glycol) microspheres containing human serum albumin. *Journal of Controlled Release*, *71*, 165–173.

Du, H. Y., & Zhang, J. H. (2010). Solvent induced shape recovery of shape memory polymer based on chemically cross-linked poly (vinyl alcohol). *Soft Matter*, *6*, 3370–3376.

Eichhorn, S., & Young, R. (2001). The Young's modulus of a microcrystalline cellulose. *Cellulose*, *8*, 197–207.

El-Sakhawy, M., & Hassan, M. L. (2007). Physical and mechanical properties of microcrystalline cellulose prepared from agricultural residues. *Carbohydrate Polymers*, *67*, 1–10.

Hu, J. L., Zhu, Y., Huang, H. H., & Lu, J. (2012). Recent advances in shape-memory polymers: Structure, mechanism, functionality, modeling and applications. *Progress in Polymer Science*, *37*, 1720–1763.

Huang, W. M., Yang, B., An, L., Li, C., & Chan, Y. S. (2005). Water-driven programmable polyurethane shape memory polymer: Demonstration and mechanism. *Applied Physics Letters*, *86*, 114105.

Jiang, H. Y., Kelch, S., & Lendlein, A. (2006). Polymers move in response to light. *Advanced Materials*, *18*, 1471–1475.

Jonoobi, M., Harun, J., Mathew, A. P., & Oksman, K. (2010). Mechanical properties of cellulose nanofiber (CNF) reinforced polylactic acid (PLA) prepared by twin screw extrusion. *Composites Science and Technology*, *70*, 1742–1747.

Kim, B. K., Lee, S. Y., & Xu, M. (1996). Polyurethanes having shape memory effects. *Polymer*, *37*, 5781–5793.

Klemm, D., Heublein, B., Fink, H. P., & Bohn, A. (2005). Cellulose: Fascinating biopolymer and sustainable raw material. *Angewandte Chemie International Edition*, *44*, 3358–3393.

Langer, R., Lendlein, A., Schmidt, A., & Grablowitz, H. (1999). Biodegradable shape memory polymers. WO Patent 1,999,042,147.

Lendlein, A., Jiang, H. Y., Jünger, O., & Langer, R. (2005). Light-induced shape-memory polymers. *Nature*, *434*, 879–882.

Lendlein, A., & Kelch, S. (2002). Shape-memory polymers. *Angewandte Chemie International Edition*, *41*, 2034–2057.

Lendlein, A., & Langer, R. (2002). Biodegradable, elastic shape-memory polymers for potential biomedical applications. *Science*, *296*, 1673–1676.

Leng, J. S., Lan, X., Liu, Y. J., & Du, S. Y. (2011). Shape-memory polymers and their composites: Stimulus methods and applications. *Progress in Materials Science*, *56*, 1077–1135.

Leng, J. S., Lv, H. B., Liu, Y. J., & Du, S. Y. (2008). Comment on "Water-driven programmable polyurethane shape memory polymer: Demonstration and mechanism" [Appl. Phys. Lett. 86, 114105 (2005)]. *Applied Physics Letters*, *92*, 206105.

Liu, C., Qin, H., & Mather, P. T. (2007). Review of progress in shape-memory polymers. *Journal of Materials Chemistry*, *17*, 1543–1558.

Liu, Y. P., Gall, K., Dunn, M. L., & McCluskey, P. (2004). Thermomechanics of shape memory polymer nanocomposites. *Mechanics of Materials*, *36*, 929–940.

Liu, Y. J., Lv, H. B., Lan, X., Leng, J. S., & Du, S. Y. (2009). Review of electro-active shape-memory polymer composite. *Composites Science and Technology*, *69*, 2064–2068.

Lu, H. B., Liu, Y. J., Leng, J. S., & Du, S. Y. (2010). Qualitative separation of the physical swelling effect on the recovery behavior of shape memory polymer. *European Polymer Journal*, *46*, 1908–1914.

Luo, X. F., & Mather, P. T. (2010). Conductive shape memory nanocomposites for high speed electrical actuation. *Soft Matter*, *6*, 2146–2149.

Lv, H. B., Leng, J. S., Liu, Y. J., & Du, S. Y. (2008). Shape-memory polymer in response to solution. *Advanced Engineering Materials*, *10*, 592–595.

Lv, H. B., Liu, Y. J., Zhang, D. X., Leng, J. S., & Du, S. Y. (2008). Solution-responsive shape-memory polymer driven by forming hydrogen bonding. *Advanced Materials Research*, *47*, 258–261.

Mendez, J., Annamalai, P. K., Eichhorn, S. J., Rusli, R., Rowan, S. J., Foster, E. J., et al. (2011). Bioinspired mechanically adaptive polymer nanocomposites with water-activated shape-memory effect. *Macromolecules*, *44*, 6827–6835.

Mohr, R., Kratz, K., Weigel, T., Lucka-Gabor, M., Moneke, M., & Lendlein, A. (2006). Initiation of shape-memory effect by inductive heating of magnetic nanoparticles in thermoplastic polymers. *Proceedings of the National Academy of Sciences of the United States of America*, *103*, 3540–3545.

Paakinaho, K., Heino, H., Pelto, M., Hannula, M., Tormala, P., & Kellomaki, M. (2012). Programmed water-induced shape-memory of bioabsorbable poly(D,L-lactide): Activation and properties in physiological temperature. *Journal of Materials Science: Materials in Medicine*, *23*, 613–621.

Passerini, N., & Craig, D. (2001). An investigation into the effects of residual water on the glass transition temperature of polylactide microspheres using modulated temperature DSC. *Journal of Controlled Release*, *73*, 111–115.

Ratna, D., & Karger-Kocsis, J. (2008). Recent advances in shape memory polymers and composites: A review. *Journal of Materials Science*, *43*, 254–269.

Schmidt, A. M. (2006). Electromagnetic activation of shape memory polymer networks containing magnetic nanoparticles. *Macromolecular Rapid Communications*, *27*, 1168–1172.

Shao, S. J., Li, L., Yang, G., Li, J. R., Luo, C., Gong, T., et al. (2011). Controlled green tea polyphenols release from electrospun PCL/MWCNTs composite nanofibers. *International Journal of Pharmaceutics*, *421*, 310–320.

Wu, Q. J., Henriksson, M., Liu, X. H., & Berglund, L. A. (2007). A high strength nanocomposite based on microcrystalline cellulose and polyurethane. *Biomacromolecules*, *8*, 3687–3692.

Xiao, Y., Zhou, S. B., Wang, L., & Gong, T. (2010). Electro-active shape memory properties of poly(epsilon-caprolactone)/functionalized multiwalled carbon nanotube nanocomposite. *ACS Applied Materials & Interfaces*, *2*, 3506–3514.

Xie, T. (2011). Recent advances in polymer shape memory. *Polymer*, *52*, 4985–5000.

Yang, B., Huang, W. M., Li, C., Lee, C., & Li, L. (2004). On the effects of moisture in a polyurethane shape memory polymer. *Smart Materials and Structures*, *13*, 191–195.

Yang, B., Huang, W. M., Li, C., & Li, L. (2006). Effects of moisture on the thermomechanical properties of a polyurethane shape memory polymer. *Polymer*, *47*, 1348–1356.

Yu, X. J., Zhou, S. B., Zheng, X. T., Guo, T., Xiao, Y., & Song, B. T. (2009). A biodegradable shape-memory nanocomposite with excellent magnetism sensitivity. *Nanotechnology*, *20*, 235702.

Zheng, X. T., Zhou, S. B., Li, X. H., & Weng, H. (2006). Shape memory properties of poly(D,L-lactide)/hydroxyapatite composites. *Biomaterials*, *27*, 4288–4295.

Zheng, X. T., Zhou, S. B., Xiao, Y., Yu, X. J., Li, X. H., & Wu, P. Z. (2009). Shape memory effect of poly(D,L-lactide)/Fe_3O_4 nanocomposites by inductive heating of magnetite particles. *Colloids and Surfaces B: Biointerfaces*, *71*, 67–72.

Zhu, Y., Hu, J. L., Luo, H. S., Young, R. J., Deng, L. B., Zhang, S., et al. (2012). Rapidly switchable water-sensitive shape-memory cellulose/elastomer nanocomposites. *Soft Matter*, *8*, 2509–2517.